# New Processing of Airborne Magnetic and Electromagnetic Data and Interpretation for Subsurface Structures in the Loei Area, Northeastern Thailand

**Kachentra Neawsuparp[a, *], Punya Charusiri[a, **] and Jayson Meyers[b]**

[a] Research Unit for Earthquake and Tectonic Geology (EATGRU), c/o Department of Geology, Faculty of Science, Chulalongkorn University, Bangkok 10330, Thailand.
[b] Exploration Geophysics, Curtin University of Technology, PO Box1987, Perth, WA 6845, Australia.

[*] Present address: Geotechnics Division, Department of Mineral Resources, Bangkok 10400, Thailand, e-mail: kachen@dmr.go.th

[**] Corresponding author e-mail: cpunya@chula.ac.th

**ABSTRACT:** The northern part of the roughly north-south trending Loei suture zone has been investigated extensively by several geoscientists for more than five decades not only for its complex geology but also for mineral exploration. In this study, we have reprocessed existing detailed aeromagnetic data for interpreting the continuity of geological units and structures where most of the pre-Cenozoic rock units are overlain by regolith cover comprised of recent soils, alluvial deposits, and colluvium surrounding hills and mountains. The aeromagnetic data were run through a series of filter routines to highlight deep and shallow magnetic features. These include analytic signal, reduction to the pole, first vertical derivative, directional cosine filtering, and upward continuation. Interpretation of all the processed geophysical data has been carried out by integration of aeromagnetic data with electromagnetic data, radiometric data, enhanced Landsat images and GIS geological information. Three geological domains (eastern, central, and western) were interpreted from the geophysical data to correspond to assemblages of contrasting rock types, as well as different regional structures identified in this study. These three domains are interpreted to be markedly separated by thrusts and sub-vertical shear zones. The magnetic data were also used to model the geometry of mafic units and granitic intrusions in 3 dimensions. Magnetic mafic bodies in the Loei suture zone were found to display their dip direction to the east. Magnetic units running along the eastern side of the Loei suture zone correspond fairly well to folded and thrust faulted basalt flows of Devonian age. Moreover, some Permo-Triassic granitoid intrusions have a strong magnetic fabric, and a few have surrounding magnetic rings are likely caused by magnetic minerals in hornfels. The others turn out to be a single smaller magnetic rings at depths suggesting only one feeding magma chamber. A few Permo-Triassic felsic to intermediate lava flows are identified by their hummocky magnetic texture. Northeast-southwest trending faults observed in the magnetic data cross-cut Triassic granite intrusions and pre-Jurassic stratigraphy, mostly producing more than 1 km of sinistral offsets. Our new interpretation agrees with the existing geological bedrock mapping in a broad sense, but shows differences in the continuity of features and extent of granitoid intrusions, and contains more large-scale structural detail. Our interpretation overlain onto the mineral occurrences map with GIS application will help to improve subsurface exploration and will help mineral explorers by highlighting new mineral target areas under thin Quaternary regolith cover.

*List of abbreviations:* GIS, Geographic Information System; DMR, Department of Mineral Resources; MRDP, Mineral Resources Devepoment Project; MORB, Mid-Oceanic Ridge Basalt; AEM, Airborne Electromagnetic Survey; TM, landsat Thematic Mapper; RTP, Reduction To the Pole; Pb, lead; Cu, copper; Zn, zinc; Au, gold; Fe, iron.

**KEYWORDS:** aeromagnetic, tectonics, lineament, structural geology, Loei.

## INTRODUCTION

Loei is a major province located in the northeastern region of Thailand, and has been of interest due to its significant mineral resources. The Loei area has been surveyed and studied extensively by several geoscientists for many decades in the contexts of geological mapping, geochemistry, structural geology

and mineral deposits. Geology of the Loei area was mapped in various scales, such as 1:250,000 by Chareonpawat *et al.*[1], 1:100,000 by Mineral Resources Development Project[2] and 1:50,000 by Chairangsee *et al.*[3]. In addition, Intasopa and Dunn[4] and Charusiri[5] dated some Triassic and Permo-Triassic igneous suites in this area by using the stepheating $^{40}Ar/^{38}Ar$ technique. Panjasawatwong *et al.*[6] studied geochemistry and tectonic setting of basaltic rocks of the Loei-Phetchabun-Ko Chang volcanic belt in Pak Chom area. Recently, Neawsuparp and Charusiri[7] studied the lineaments determined from the enhanced Landsat TM5 in the Loei and nearby areas. Seusutthiya and Maopeth[8] studied petrography and whole-rock geochemistry of some ultramafic rocks in Ban Bun Tan, Suwan Khuha area of Nong Bua Lumphu Province, east of the Loei area.

The Loei area has been selected for mineral deposit investigation by using airborne geophysical surveys performed by the Department of Mineral Resources (DMR) since 1987[9]. Helicopter airborne geophysical surveys flown at 60m terrain clearance and 400m line spacing measuring electromagnetic (AEM) and magnetic fields were conducted by Kenting Earth Science International Limited (KESIL), Canada, in 1987-1988. Subsequently, these airborne geophysical data were used in several aspects, such as mineral exploration[9-10] and preliminary structural interpretation in the Loei area[11].

Galong and Tulayatid[9] used the processed airborne electromagnetic data for assisting in geological mapping in the eastern part of the Loei area. Rangubpit[10] applied image processing and interpretation of aeromagnetic for geological mapping in Ban Yuak and Ban Sup, located between Loei and Udon Thani provinces. However, these two research works delineated simple geological boundaries, and suggested the occurrences of possible mineral deposits.

Tectonically, the Loei area is situated in the "Loei Fold Belt"[12] or the easternmost part of the Nakhon Thai tectonic block[13]. Very recently, Charusiri *et al.*[13] proposed that the eastern Loei suture, within the Loei area, forms the boundary between the Indochina and the Nakhon Thai tectonic plates (Fig. 1A). However, the Loei suture is poorly studied and difficult to delineate due to the fact that some parts of the suture (or "tectonic lines") are underneath thick regolith cover or Jurassic to recent sedimentary covers.

Though the Loei area has been surveyed and studied by several geoscientists, particularly for the surface geological mapping. The subsurface geologic mapping has never been performed by integrating geological and geophysical results, and no attempt has been made so far to understand the detailed relationship between structural features observed on the ground and those extending into the subsurface.

This paper is aimed at re-processing aeromagnetic data to study major surface and subsurface structures, and their relationship with surface structural features in the Loei study area. A new interpretation map has been generated showing magnetic units and structures, and the model of subsurface structures are presented
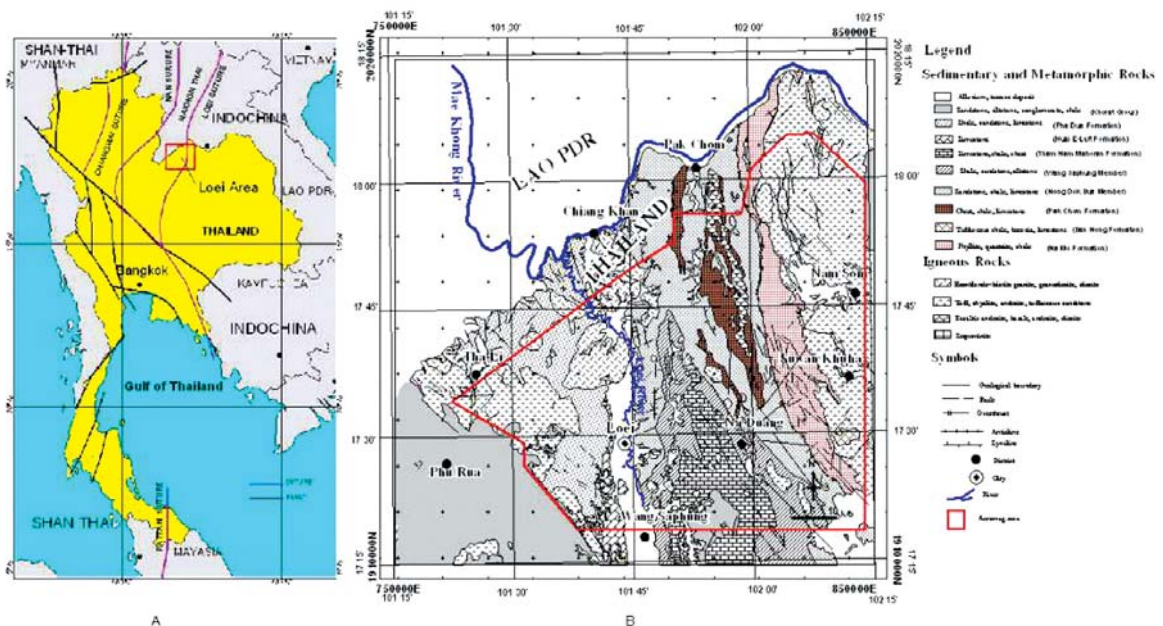


**Fig 1.** (A) Map of Thailand and adjoining countries showing tectonic blocks and sutures (modified after Charusiri *et al.*[13]). Note that the inset is the study area.
(B) Geologic map of the Loei study area, northeast Thailand (modified after MRDP[2] and Chairangsee *et al.*[3]).
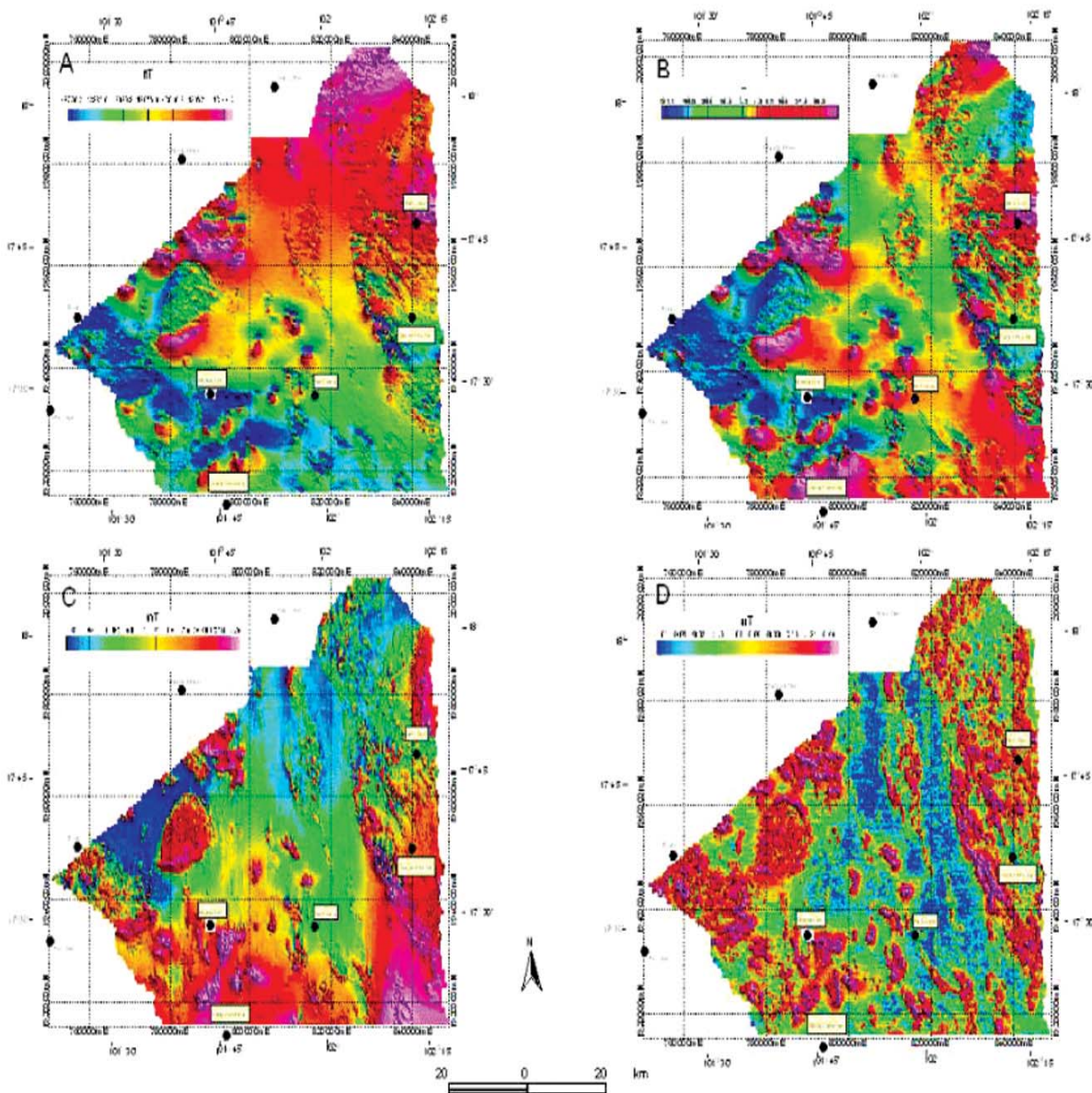
**Fig 2.** Aeromagnetic data processing maps of the Loei study area based on (A) total magnetic intensity data, (B) residual magnetic intensity data, (C) reduction to the pole (RTP) data, and (D) analytic signal data.

and discussed.

The area under investigation, covering about 5,280 sq km, is located at latitudes 17° 15' to 18° 15' N and longitudes 101° 15' to 102° 15' E. The study area encompasses the northern and eastern parts of Loei and the western part of Nong Bua Lumphu provinces in northeastern Thailand, close to the Thailand and Loa PDR border (Fig. 1A).

## GEOLOGIC SETTING

The regional geologic setting of the Loei area shown in Fig. 1B is summarized from the reports of Bunopas[14]

at 1:100,000 scale and of Chairangsee *et al.*[3] at 1:50,000 scale.

Rock sequences commence with Middle Palaeozoic metamorphic rocks containing very rare and poorly defined fossils, which mainly include quartzite and phyllite in the eastern part of the Loei area. These metamorphic rocks are unconformably overlain by alternated strata of shale and siltstone with tuff and intercalated limestone. Intensely folded chert beds with interbeds of thin volcanic clastic rocks of Upper Paleozoic age are restricted to the central part. The chert unit is situated adjacent to spilitic basaltic rocks with the age ranging from Devonian to Carboniferous[4].

Both chert and basalt units form a long, narrow north-south trending belt in the central part of the study area. This basaltic unit extruded onto the sea floor forming huge masses of volcanic tuff and pillow lava associated with sporadic manganese deposits. In the Late middle Devonian to Carboniferous, thick sequences of greywacke intercalated with shale and reef limestone were observed in several places. Late Palaeozoic reef limestones lie unconformably over the older rocks. Permo-Triassic felsic tuff, such as rhyolitic tuff, covers a large area located mostly in the eastern part of the study area, whereas andesitic rocks with Cu-Pb-Zn-Au mineralization cover in the western part of the investigated area. Granite and granodiorite of Triassic age, with associated Cu-Fe-Au skarn/porphyry-type mineralization[5, 13], are located in the western part of the area.

In the Loei study area, the major structural features are folds and faults. The main faults and fold axes are oriented in a north-south direction. Additionally, Bunopas[14] and Chairangsee *et al.*[3] reported unconformities in the mapped area between strata of different ages, for example, between Permian and Late Triassic and between Lower Carboniferous and Devonian. However, they are poorly stratigraphically and structurally defined due to discontinuous exposures between rice fields and alluvial cover, and thick natural vegetation with soil cover.

We regard the Loei study area as part of the recognized " Loei Fold Belt"[12], which corresponds to the Loei-Phetchabun–Ko Chang Volcanic Belt[15]and the Eastern Granite Belt of Thailand[16]. Large anticlines and synclines with axes mainly trending in a north-south direction occur in Silurian and Permian rock sequences. Many folds are dislocated by several sets of strike-slip faults oriented in northeast-southwest and northwest-southeast directions. These faults seem
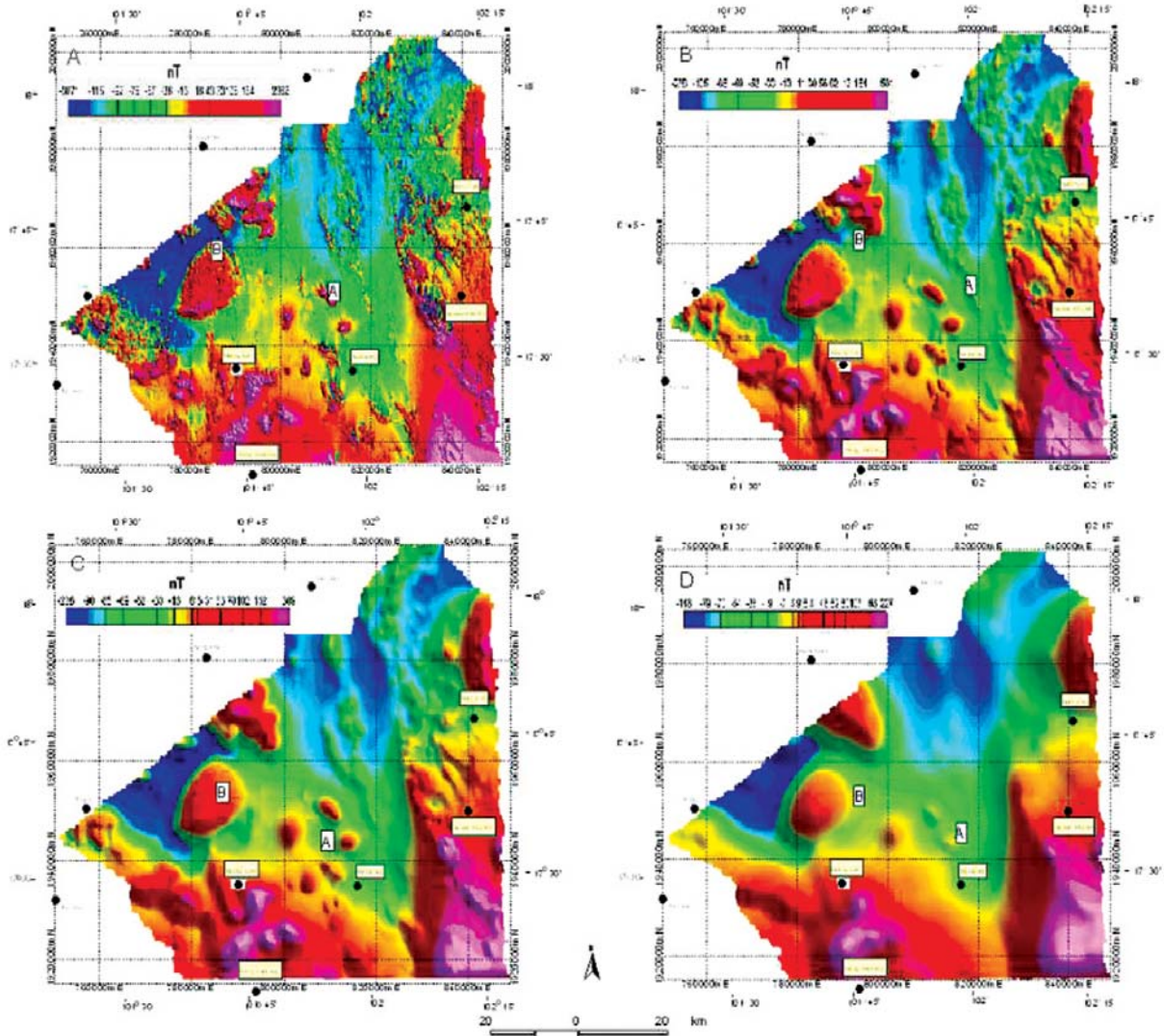


**Fig 3.** Enhanced RTP maps of the Loei study area, with upward continuation (A) at 50 m, (B) at 500 m, (C) at 1000 m, and (D) at 3000 m.

**Fig 4.** Enhanced aeromagnetic and electromagnetic maps of the Loei study area using (A) first vertical derivative technique, (B) directional cosine filtering in north-south direction, (C) AEM data of frequency 912 Hz, based on in-phase component, and (D) AEM data of frequency 912 Hz, based on quadrature component.

dominant, and dislocate major folds and pre-existing thrust faults. Sinistral movement, which is more common than dextral movement, is present especially in the western part of Loei. This is probably due to the continuous clockwise rotation of continental Southeast Asia[12,13]. The large, north-south trending overthrust in the eastern part of Loei area separates Silurian-Devonian metamorphic rocks from Carboniferous sedimentary rocks[9].

## MATERIALS AND METHODS

### Data Sets

The main data set used in this study is an airborne geophysical survey data acquired during 1987-1988 by KESIL with the contract from DMR through MRDP. This survey  measured high-resolution AEM and magnetic responses over the northern part of Loei and nearby Nongbua Lamphu provinces.

In this study, we used the aeromagnetic and electromagnetic data for a total of 13,256 line-kilometers. The survey was traversed by helicopter flown in an east-west direction, with a line spacing of 400 m and at an altitude of 60 m above the ground level to cover an area of 5,280 square-kilometers.

Beside the aeromagnetic and AEM data, we used radiometric, digital elevation, Landsat TM5 and available GIS data, both published and unpublished, for integration and interpretation.

A revised geological map compiled from the geological maps on scales of 1:100,000 by MRDP[2] and 1:50,000 by Chairangsee *et al.*[3] was used to compare with the interpreted geophysical map. In addition, the detailed studies of igneous rocks in the area[4,5,6,8] were also evaluated for visualizing and classifying magnetic domains.

Lineament studied in the Loei area from remote-sensing interpretation[7] was used to discuss with the geophysical lineaments generated from this study. Moreover, the interpreted AEM, magnetic and radiometric data in some parts of the Loei area[9,10] were also applied to add subsurface information in this study.
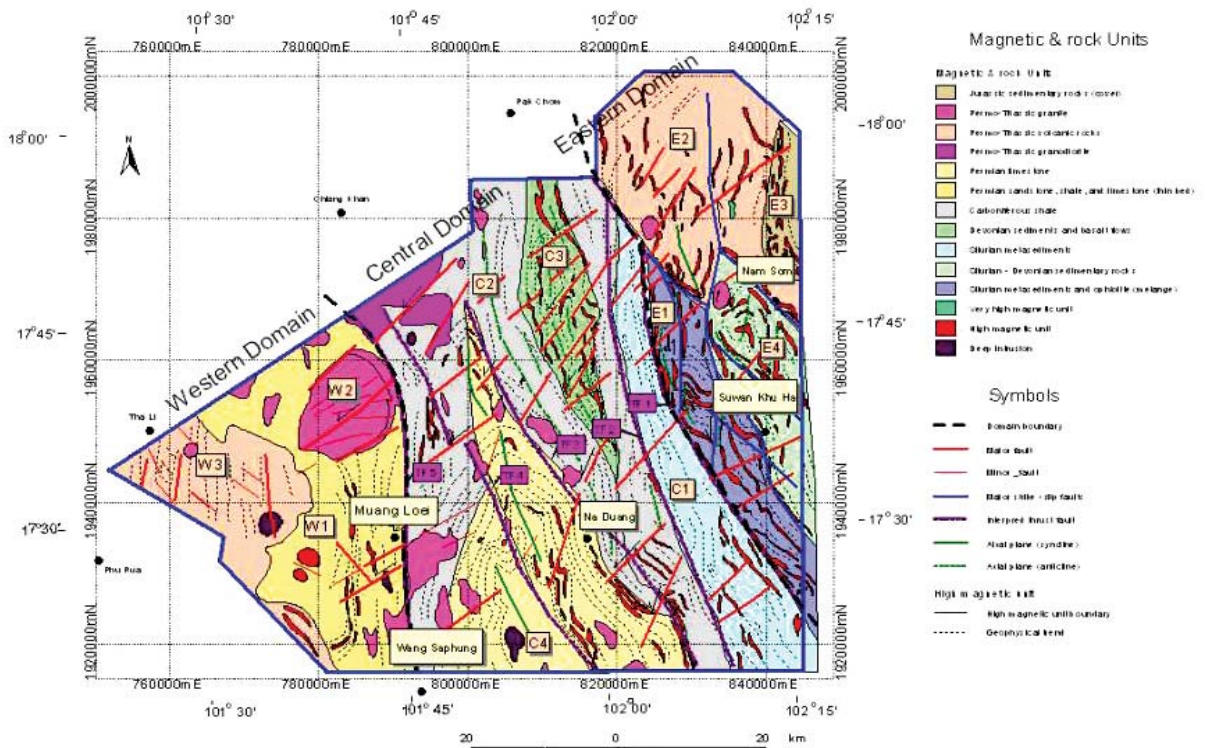
**Fig 5.** Geophysical interpretation map of the Loei study area showing eastern, central, and western magnetic domains and their associated subsurface structures.
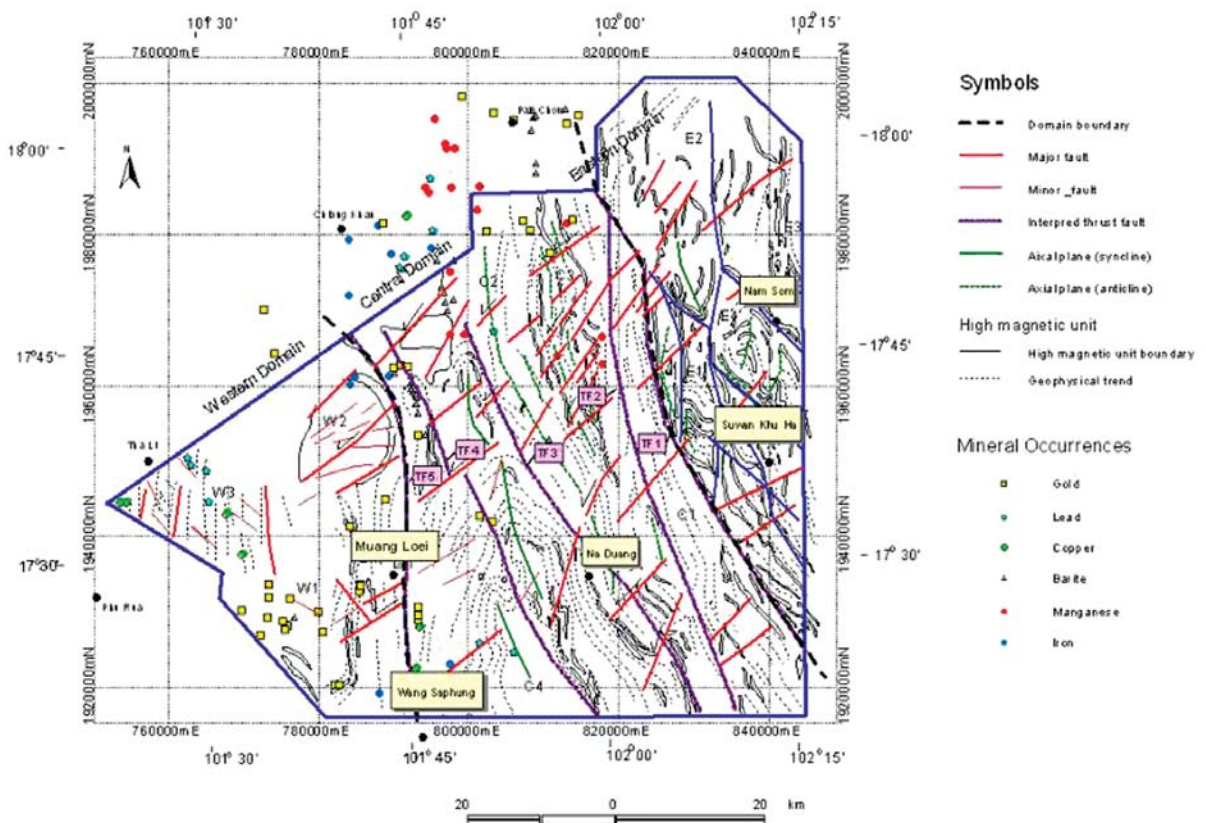


**Fig 6.** Geophysical lineament map with significant mineral occurrences in the Loei study area.

Several works on tectonic evolution, such as Bunopas[12] and Charusiri *et al*.[3], were used to redefine the tectonic elements from the geophysical information.

## Aeromagnetic Processing Methods

Aeromagnetic data provides the most significant information for subsurface interpretation. Therefore, the methodology is explained in detail. Total aeromagnetic data recorded in analogue form were digitized as profile data. Magnetic intensity generated from the profile to grid data was then displayed as an image in natural color pallets (magenta high intensity, blue low intensity, see Fig. 2A), using histogram equalization to maximize the color ranges. To emphasize the expression of anomalies near surfaces, the color-shade grid with illumination inclination and declination at 45° is displayed.

In this study, it is essential to define the magnetic anomalies at the place where they sit over the source, because there is a considerable difference in magnetic intensities from the inclination and declination at low latitudes. By removing the International Geomagnetic Reference Field (IGRF), residual magnetic data (Fig. 2B) can be either positive (higher than the IGRF) or negative (lower than the IGRF) depending on the orientation of each magnetic body, but distortions in the normal response still remain.

Mathematical transformation or filtering techniques, such as reduction to the pole (or RTP, Fig. 2C), analytic signal (Fig. 2D), upward continuity (Fig. 3), vertical derivative (Fig. 4A) and directional cosine filtering (Fig. 4B), were applied to the magnetic data to enhance features for interpretation. The individual transformation techniques are explained in more detail in Neawsuparp[17]. In this current study, we adopted and slightly modified the methodology described by Milligan and Gunn[18].

Many of the linear anomalies for the Loei area were not completely revealed by shaded-relief total magnetic imagery. Interpretations using vertical derivative plus automatic gain control methods remove the influence of the large amplitude, long wavelength anomalies. The directional cosine filter method, in particular, worked well to reveal a comprehensive pattern of faulting within the basin fill[19]. Upward continuation filtering helped determine the depth range of deeper sources. All the methods together provided a view of the pattern and general depth ranges of intra-basin faults within the area that aid research on the geology, intrusions, and faults with respect to the mineral resources.

## Electromagnetic Processing Methods

Electromagnetic data recorded in the frequency domain are divided into 4 channels. including x and y in-phase and quadrature for the frequencies: 736, 912 and 4200 Hz. In-phase and quadrature data were converted to apparent resistivity for 4200 Hz. The data processing of AEM data were displayed in grid images that can be overlaid with the other data by using GIS (Arcview version 3.2 program).

All data were moved to the zero level. This technique was applied to decrease the leveling problems. In order to create grid, we used the spline grid method because this grid method has been useful for the wide line spacing data and for reducing the trend enforcement gridding problem.

Apparent resistivity grids were imaged as conductivity grids. Additionally, since anomalies in AEM showed negative amplitudes, the in-phase and quadrature data were multiplied by -1 to convert the data to high amplitude anomalies. The electromagnetic data of 912 Hz were displayed as in-phase and quadrature components (Figs. 4 C and D, respectively).

## Interpretation Method

Visual interpretation was made on hard copies for all geophysical data processed at 1:100,000 scale, to diminish parallax problems caused by computer displaying. The boundaries were then mapped more accurately using the source edge maps by placing margins at the position of the source edges coinciding with major amplitude change. The interpreted aeromagnetic and AEM data were integrated with others GIS data for mapping geological structures and continuity of lineaments, which represented faults and folds in the study area. Domain boundaries and structural features, such as folds, faults and thrusts, and their relations to intrusions, were also digitized (Fig. 5).

From the interpretation map, the subsurface modeling of the area was created by using the ModelVison software in both forward and inversion modeling methods. Magnetic response profiles of the reduction to the pole were selected for modeling. To simplify models, line profile and cross sections were constructed based on latitudes of the area and the locations of latitudes were used for the name of line profile. We applied three profile lines for magnetic modeling including L1920000N, L1950000N and L1970000N in the east-west direction (Fig. 7).

Magnetic modeling in this study was used for both of linear inversion and non-linear inversion methods. The linear inversion technique[20] involves subdividing the space below an observed magnetic field into series of geometric bodies and then finding values of magnetization for the shapes in such a way that the summed magnetic effect of all the bodies matched the observed magnetic field. The non-linear inversion technique was applied in an attempt to obtain a match between observed and calculated magnetic fields by
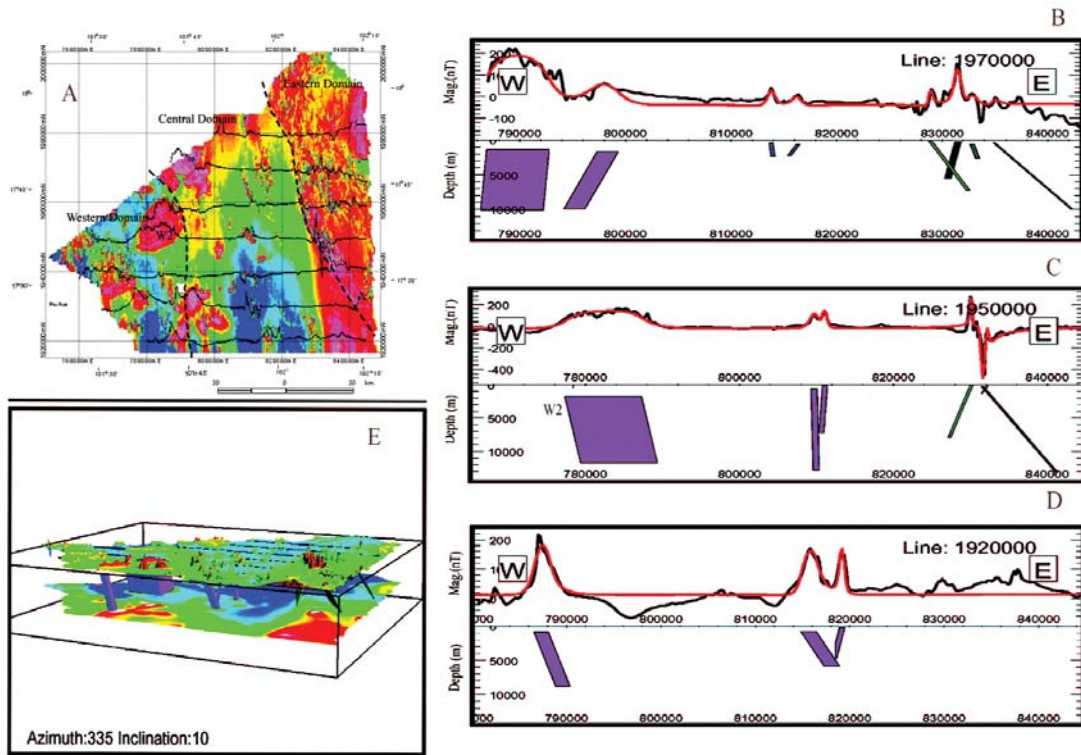
**Fig 7.** Aeromagnetic modeling of the Loei study area showing (A) selected aeromagnetic line at different latitudes displaying on the RTP map, (B) cross-section along the line L 1,920,000N, (C) cross-section along the line L 1,950,000N, (D) cross-section along the line L 1,970,000N, and (E) 3D perspective view in azimuth 335 °and inclination 10° showing interpreted subsurface magnetic structures.
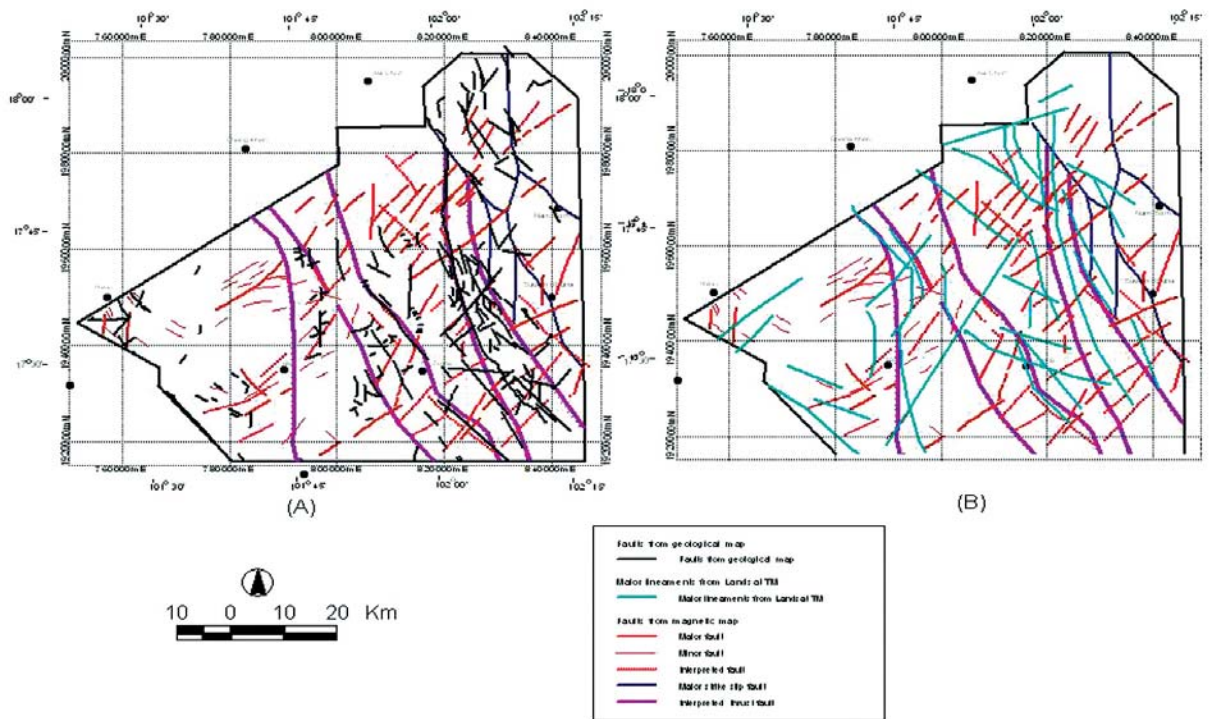


**Fig 8.** Lineament maps of the Loei study area showing structural patterns in comparison with (A) major faults from the geological map (Fig. 2), and (B) patterns from the enhanced Landsat map[7], with new structure and domains from the geophysical interpretation.

iteratively varying the unknown parameters. Using a trial and error method, variations that improved the fit between the observed field and calculated results based on the model were stored and used as a basis for new parameter estimating[19]. In this study, the forward model is initially obtained to best fit between the observed and calculated magnetic field. Then the inversion to produce the final perfect fit by interactive modeling was applied.

## RESULT AND INTERPRETATION

### Results

The total magnetic field (Fig. 2A) shows regional high magnetic intensities in the northern part and low intensities in the southern part of the Loei study area. After we removed the IGRF from the total magnetic field, the result is a residual magnetic map (Fig. 2B) showing the difference in locations of high and low magnetic intensities. The relative residual magnetic map (IGRF-corrected) shows a rather complex crustal magnetization pattern. Magnetic intensity level ranges from -820 to 980 nT, with a base level of -4.25 nT. Local variations of field intensity always exceed 500 nT in the eastern part and diminish rather abruptly to less than 100 nT in the central and northwestern parts.

The residual magnetic intensity map (Fig. 2B) exhibits three regional magnetic zones that roughly trend in a north-south direction. From the east, there exists a high magnetic intensity zone clearly visible on the enhanced map. The most prominent low magnetic intensity zone is in the central part, between Na Dung and Pak Chom districts, and continues northward to the Pak Chom district and Lao PDR. Within this zone, there are series of elongated and relatively higher magnetic intensities trending in a northwest-southeast direction. Additionally, the boundary between the central zone and the eastern zone is displayed by a fairly sharp magnetic contrast. To the west, the zone is characterized by groups of strong, positive, and roughly circular anomalies (approximately 2 km in diameter). These are located in the southern part, whereas in the north, the large circular features have an average diameter of about 10 km.

Both RTP (Fig. 2C) and analytic signal (Fig. 2D) maps display similar magnetic features and such enhancements lead to more outstanding magnetic boundaries. The RTP map shows the average peak to peak at about 700 nT. These high anomalies are oriented in a north-south trend, with a total length of about 40 km. The western edge of this anomaly is marked by a sharp magnetic gradient in a northwest-southeast trend, extending from Suwan Khuha district to Nam Som district (in Nong Bua Lumphu province). The analytical signal image shows the marked narrow zone

between the eastern and central parts better than those of the previously described images. It should be emphasized that the boundary contrast within individual zones is quite clear.

The filtered images following RTP and upward continuation (Figs. 3) show the high magnetic anomalies varying in geometry and locations at different depth. For example, groups of circular features in the central part (A in Fig.3) are changed to the small circular magnetic body in the deeper part whereas the large circular magnetic body (B in Fig. 3) in the western part remains similar in size and geometry.

The first vertical derivative (Fig. 4A) and the directional cosine filter (Fig. 4B) maps reveal a significant magnetic pattern, such as linear structures, better than those of the other maps. As shown in Fig. 4A, linear patterns are more prominent in the east than in the central and western parts. Most of these are steeply dipping vergence volcanic horizons. However, the linear patterns in the west can be better defined using the directional cosine filter (see Fig. 4B). Application of the directional cosine filters of total magnetic maps in the north-south direction shows well-defined lineaments, particularly those trending in the northeast-southwest direction. The long and continuous lineaments of this direction seem to cross-cut three regional magnetic zones earlier mentioned. Additionally, some lineaments, such as those in the south of Pak Chom district, show minor displacements (less than 0.5 km). The results shown in these maps clearly indicate that most of the northwest lineaments are cross-cut by the northeast-southwest trending lineaments.

### Interpretation

From the results of enhanced aeromagnetic maps we were able to distinguish the magnetic responses in the bedrock geology due to the difference in magnetic susceptibilities, structures and deformation styles of the magnetic units in the area. Variable source depths within a domain may also contribute significantly to changes in anomaly sizes and shapes sizes.

### Magnetic Domains

From the enhanced image maps, we created a new interpretation map shown in Fig. 5. With data integration and interpretation, we divided the Loei study area into three magnetic domains based upon the magnetic intensities, structural styles, and geological features, namely Eastern, Central, and Western domains. Boundaries of the individual domains clearly coincide with the abrupt changes in average magnetic intensities, anomaly variabilities and orientations. Each domain was further divided into sub-domains on the basis of local detailed magnetization, interpreted

subsurface geology and structure, lineament patterns, and circular features described in the previous section. The characteristics of individual sub-domains are described by comparing the interpretation with proposed geological features (see Fig. 1B).

*Eastern Domain*

The eastern domain is the geophysical domain clearly trending in an almost north-south direction. The sharp boundary between the eastern and central domains is regarded as a shear zone. It is chiefly composed of moderate to high magnetic intensities of volcanic rocks. Our field investigation revealed the very high magnetic intensity units in the southwestern part corresponding to the newly exposed mafic and ultramafic rocks. These rock units are not shown in any previous geological maps (Fig. 1B). We further divided the eastern domain into four main sub-domains namely E1, E2, E3 and E4 sub-domains, based on the average magnetization and structural styles.

The E1 sub-domain shows the highest magnetic intensities and is located in the southwestern part of the domain. Our field investigation and recent petrographical studies[8] indicate the occurrences of serpentinized ultramafic rocks. These serpentinized rocks account for nearly 70 percent of the E1 sub-domain. Shear zones are the main deformation structures, commonly exceeding 40 km in length and mostly trending in a north-south direction. The shear zones are characterized by overlapping lineaments, and form the 'S' shaped curvi-lineaments from folding and thrust. Structural geophysical trends within these ultramafic rocks are largely aligned to the north and northwest trends. In addition, intense folds of variably magnetized strata, shown as curved and banded magnetic patterns, are observed in the southern part. Such banded patterns are quite similar to those interpreted to represent folded structures of sedimentary rock strata in Finland[21]. A series of interpreted synclines and anticlines show the average north-south trending axial plane. Two strike-slip faults, of similar trend, are also recognized in the northern part of the E1 sub-domain, and they show minor left lateral movement of about 0.5 km.

The E2 sub-domain is located in the northern half of the domain. This sub-domain is characterized by low to moderate magnetization corresponding to the felsic volcanic rocks (rhyolite and rhyolitic tuffs), as well as granite plutons mapped by Chairangsee *et al.*[3]. This sub-domain may be related to the E1 sub-domain with a shear contact at depth and ultramafic rocks are apparent contact of the boundaries between E1 and E2 sub-domain.

The E3 sub-domain is located in the northeastern part of the eastern domain. This sub-domain is dominated by a large circular high magnetic unit with a north-south structural trend. In the geological map, this sub-domain is mapped as Mesozoic continental sedimentary rocks of the Khorat Group, which has low magnetization. The contrast in the magnetic responses leads us to believe that there are some felsic intrusions underneath these non-marine strata.

The E4 sub-domain is located in the eastern part of the domain, and displays moderate magnetic intensities. They are interpreted to represent sedimentary rocks underlying the E2 felsic volcanic rocks. A syncline, as indicated by a high magnetic unit, has a length of about 10 km, and its axial trace trends in a north-south direction. The E4 sub-domain is separated from the E2 sub-domain by a strike-slip fault.

*Central Domain*

The central domain is largely composed of low magnetic intensity features. It can be divided into four sub-domains namely C1, C2, C3 and C4 sub-domains using magnetic shape, pattern, and intensities, as well as distribution of small magnetic intensive stocks.

The C1 sub-domain forms a north to northwest-southeast trending low magnetic zone, and corresponds to thick meta-sedimentary rock sequences with mostly the northwest strike[2, 3]. These metasediments were obviously affected by tectonic deformation and metamorphism much more intensely than any other rocks in the Loei area. The second oldest sedimentary rocks of Ban Nong Formation have a definite age of Silurian-Devonian by using the evidence of several corals such as Heliolites sp, H. barrandei and Favosite sp[22]. Thus, the metamorphic rocks were at least of middle Silurian in age[3]. This sub-domain shows several long, north to northwest-southeast trending magnetic linear patterns interpreted to be associated with major faults running parallel to a regional structure. These faults are up to 30 km long and are identified clearly by the AEM image data[17], because the extension of poorly magnetized faults with similarly magnetized sedimentary rocks is difficult to determine from the processed aeromagnetic data. To the south of the sub-domain, a series of AEM conductive zone occurs following the major fault trend.

The C2 sub-domain is dominated by a low magnetic pattern with lineaments similar in style to those of the C1 sub-domain. In the western part of this sub-domain, to the north of Na Duang, circular magnetic highs indicate intrusive stocks. This sub-domain was mapped as Carboniferous clastic sequences of the Wang Saphung Formation[3]. The circular magnetic anomalies observed in the central part were mapped as the felsic intrusive bodies[3]. As shown in Fig. 5, the boundary between C1 and C2 sub-domains is marked by a major north-south trending thrust fault. To the west, the

north-south trending anticline is dominant.

Embedded into the C2 sub-domain, in a roughly north-south direction, is the C3 sub-domain, which consists of an elongate high magnetic intensity trend. This sub-domain is equivalent to the mafic volcanic belt of basalt to basaltic andesite in composition[3]. This high magnetic unit shows many short northeast- southwest trending lineaments with a series of intricate folds in the same trend, and two small thrust faults in the north-south direction.

The C4 sub-domain is mainly composed of low magnetic intensities. This sub-domain corresponds to thick Permian carbonates and clastic sequences of the Loei Group. The-long wavelength regional folding probably resulted in a symmetrical variation of magnetic field intensity[23]. The clearly defined lineament trend is illustrated by the curved lineament patterns (see Fig. 6) interpreted to represent a large folded structure with the regional axial plane in the northwest trend. The boundary between the C2 and C4 sub-domains is interpreted to follow thrust faults trending in a northwest direction.

*Western Domain*

The western domain is essentially composed of moderate magnetization. This domain is divided into three sub-domains namely W1, W2 and W3 sub-domains) based on high magnetic patterns and intensities. The boundary between the central and western domains is characterized by a north-south trending thrust fault.

The W1 sub-domain is indicated by moderate magnetization corresponding to the Permian sandstones with interbedded limestone[3]. Geologically, this sub-domain shows a structural trend in a north-south direction similar to that of the regional mapped rock units.

Enclosed by the W1 sub-domain in the northern part, the W2 sub-domain shows a large circular high magnetic pattern (10 x 15 km in size). This sub-domain is cross-cut by northeast-southwest trending major faults. In the field, this sub-domain is comprised of felsic plutonic rocks.

The W3 sub-domain consists of moderate to high magnetization with a straight linear pattern in a north-south direction. This sub-domain is interpreted to represent intermediate to mafic volcanic rocks, mainly andesite[2]. There are a few small circular features, possibly suggesting volcanic vents occurring in the eastern and western parts.

## Magnetic Structures

Fig. 6 displays major lineaments of various patterns and styles drawn using interpretation following the image manipulation. The lineaments were interpreted on the enhanced airborne geophysical data from visual hard copy images on a 1:100,000 scale. Geologic lineaments (fractures and faults) were superimposed afterward as a separate layer. Comparison with the geologic lineaments shows that many of the magnetic anomaly trends coincide with geological contacts or faults.

The eastern domain is characterized by a rather irregular pattern of magnetic anomalies containing long segments having predominant north-south linear trends. This belt was separated by the sharp, long, northwest-southeast lineaments conformable with regional structures. These lineaments show the strike-slip fault motion indicated by the displaced lineaments and rock units, and some lineaments were interpreted as shear zone by high magnetic units with the 'S' shaped features. The magnetic data also show small folds consisting of several discontinuous, dextrally side-stepping lineaments with displacement of about 1 km. The structural pattern of this belt shows that the major structures were formed in response to compressional tectonic activity in the region. Moreover, the magnetic lineaments can be inferred as axial planes of some of the folds. Good examples are those in the E4 sub-domain, with north-south trending and northeast-southwest trending.

The central domain comprises sets of northeast-southwest trending structural patterns. The prominent features are characterized by the large-scale, open and upright folds in the northern and southern parts, which are obvious in both magnetic and geologic maps. In the northern part, steeply-dipping and tightly-folded sedimentary strata of Devonian age are mapped within the area with low magnetic intensities. This zone forms a rather strong lineament pattern along most of its length and cross-cuts the set of folds. In the southern part, dominant northeast-southwest trending lineaments are clearly visible and form large fold structures.

The boundary between the central and eastern domains is mapped as the thrust fault by MRDP[2]. In the geological map, the thrust marks the boundary between the metamorphic rocks and sedimentary strata of different ages. But our aeromagnetic result shows no contrasting signature at the western and eastern sides of the fault boundary. However, from the processed aeromagnetic interpretation, a consistent sharp and strong magnetic gradient was observed at the boundary near the mapped thrust fault, which is about 5 km to the east. However, some faults in the Loei basin area have either no magnetic expression or such a small one that it was not detected by aeromagnetic data. In addition, the extent of poorly magnetized shear zones and faults yield similar values of magnetization to sedimentary rocks, so they are difficult to be determined

from the aeromagnetic data. In these cases the AEM maps are used to delineate the shear zones and faults in the study area. Our AEM interpretative result (see Figs. 4C and D) shows the long lineament pattern of high conductors at the same location of the mapped thrust fault as shown in the Fig 5 and 6.

To identify a thrust fault by using geophysical data, seismic and gravity data are commonly used for observing faults and their dips.

Pluijm and Marshake[23] reported that fault systems were common along the tectonic margins of convergent plates, and faults tend to be composed of relays or parallel arrays. In addition, Airo and Ruotoistenmark[21] discussed that thrust faults were typical geological boundaries that separated regions or geological blocks showing different deformation styles and structures. Thrusting, which follows the main deformation stage, was recognized as abrupt termination of one deformation style with regard to the adjacent one. Moreover, regions of folding were often separated by large-scale fault zones or thrust faults running parallel to the axial-plane strike or groups of smaller faults with the same trend. Therefore, in this study, five thrust faults with a length of 20 to 60 km were interpreted based on the magnetic patterns and geological characteristics.

Fig. 5 and 6 show the interpreted thrust faults (TF) from the interpretation of aeromagnetic and electromagnetic maps. The TF1 and TF2 represent the boundaries between eastern and central domains, and between central and western domains, respectively. The TF2 is interpreted as the thrust fault conforming to the geological map[2, 3]. The TF3 separates a series of small tight anticline folds in the eastern side (C2 and C3 sub-domains) and a large open syncline fold in the west (C4 sub-domain). The TF4 represents a series of thrust faults separated the large open fold in the C4 sub-domain, which parallels the axial-plane strike, and developed during folding.

Small northeast-southwest trending lineaments are dominant in the western domain, with geophysical trends in a north-south direction. In Fig. 5 the boundary between central and western domains are interpreted from contrasting magnetic patterns. The prominent structure of this domain is a large circular feature, similar to the mapped Triassic granite intrusion. Additionally, this circular structure was cross-cut by the northeast-southwest trending lineaments, suggesting that the northeast lineaments are of younger age than the granite intrusion.

### Magnetic Modeling

From the results of magnetic data interpretation, we were able to construct a geophysical model for both forward and inversion methods. In this study, magnetic response profiles from the RTP data were selected for modeling. To simplify the line profiles, cross sections were draw based on latitudes of study area (Fig. 7A). Three profile lines in the east-west direction were selected for modeling, including line numbers L1920000N, L1950000N and 1970000N.

Fig. 7A shows the selected RTP aeromagnetic data along the east-west surveyed line with data interpretation. Three cross-sections along the lines L1970000N, L1950000N and 1920000N are illustrated in Figs. 7B, C and D, respectively. In the western side of the study area (at grid coordinate 790000E-800000E), interpreted bodies have magnetic intensity higher than those of the surrounding areas, suggesting magnetic intrusions/ or dikes of possibly granitic composition. The circular feature (W2) in the western domain is the largest body, which is east-dipping at depth. On the surveyed line L1970000N (Fig. 7B) at coordinate 815000E, small dike-like bodies are indicated by high magnetic intensities, corresponding to the volcanic (basalt) unit (C3) of the central domain. At grid coordinate 830000E-835000E along the lines 1950000N and 1970000N (Figs. 7B and C), a series of narrow magnetic dikes are encountered, and they are interpreted to represent the east-dipping faults whereas the west-dipping dikes correspond to the mapped ultramafic rocks. These anomalies are interpreted to be related to the fault zone with northwest-southeast trend, and contain mainly ultramafic and meta-sedimentary rocks in the eastern domain (E1). This assemblage probably represents a melange of ophiolite crust.

A perspective view in 3 D is displayed in Fig. 7E in the azimuth and inclination at 335° and 10°, respectively. The model is a result of the overlaying maps of the RTP grid at the top surface, and upward 1,000 meters at the bottom. The model shows that magnetic bodies continue to the deeper zone.

## DISCUSSION

### Magnetic Responses Related to Rock Units

To correlate magnetic anomalies with rock units, it is noteworthy that sedimentary rocks are generally not magnetic, whereas igneous rocks rich in iron and magnesium (mafic to ultramafic) tend to be very magnetic. Granite intrusions and hornfels contact aureoles can also be magnetic.

Magnetic quiet areas are widely distributed in the central and northwestern parts of the study area and exhibit magnetic relief of 50 nT or less. These areas correspond to a basin filled with Carboniferous clastic and Devonian chert sediments[3]. These areas are faulted and folded as recognized both in the field and in the geophysical and Landsat imagery interpretation map.

Meta-clastic rocks in the westernmost part (the C1 sub-domain) also have low magnetic intensities similar to those of the Carboniferous sediments. Moreover, results on magnetic susceptibility indicate that several rock samples yield rather low values[17]. However, it is generally accepted that metamorphic rocks have more magnetic susceptibility than sedimentary rocks (average sedimentary and metamorphic rocks about 75 emu and 350 emu, respectively, Telford et al.[24]). We, therefore, consider that the meta-clastic unit (in the C1 sub-domain) is likely to be the same geologic unit as the Carboniferous clastic unit. Otherwise, magnetic mineral contents decrease accompanying collisional process[25]. Either burial pressure-dominated or weak dynamo-thermal metamorphism of Late Paleozoic clastic rocks associated with folding and thrusting may have formed in response to compressional tectonics, similar to that occurring along the Nan Suture.

The magnetically moderate areas have accentuated magnetic relief with lineaments and anomalies having amplitudes of 100 to 400 nT. Most of the magnetic anomalies in these areas are observed over plutonic rock exposures. Magnetic field intensity increases by more than 200 nT over a poorly exposed granodiorite stock. The small circular magnetic bodies in the southern part of the study area suggest that these features are caused by intrusive rocks, corresponding well with several of the known granodiorite stocks. Moreover, the results of this study show more extent and new granitoid intrusions than the previous geological mapping (see Figs. 1B and 5).

Narrow and higher amplitude anomalies in the north of the central part (the C3 sub-domain) indicate the existence of mafic volcanic rocks corresponding to Carboniferous basalt and basaltic andesite[2, 3]. The volcanic rocks (the C3-sub-domain) are made up mainly of pillow lava, hyaloclastites and pillow breccias. These volcanic rocks have been assigned to those erupted in a mid-ocean ridge to back arc basin environment, and have a wholerock Rb-Sr Isochron age of 341 ±11 Ma[4]. Geochemical results from the volcanic rocks in the Loei area by Panjasawatworng et al.[6], suggest that the Loei volcanic rocks are comprised of MORB and oceanic island-arc lava.

Additionally, volcanic rocks in the north of the E2 sub-domain show lower magnetic intensities than the volcanic rocks in the W3 sub-domain. Based on our field visits and geological maps by MRDP[2] and Chairangsee et al.[3], the volcanic rocks of the eastern part are dominated by more felsic variations and those of the western part are characterized by more mafic variations.

The magnetically high areas of the E1 sub-domain show magnetic anomalies with amplitudes of more than 500 nT, and are characterized by high wavelength anomalies. Large anomalies are situated close to the border of metamorphic and volcanic rocks in the southeastern part of the studied area. The magnetic intensities in this zone are higher than those of the metamorphic and volcanic rocks. It is very interesting that this zone is not shown in the geological map. These strong magnetic anomalies are oriented in a northwest-southeast direction. The surface geology mapped by MRDP[2] and Chairangsee et al.[3] does not show an obvious cause of the high positive magnetic anomalies. The results of our and previous field data indicate that these intense anomalies correspond to the mapped mafic and ultramafic intrusions comprised of serpentinite, peridotite and gabbro[8]. The studies of petrological and geological characteristics of serpentinized rocks[8] suggest that these rocks were retrograded or hydrothermally metamorphosed from dunite, pyroxinite and peridotite.

There are some correspondences between the high, elongated magnetic zone and outcropping serpentinites along a fault in the vicinity of Ban Bun Tan, Suwan Khuha District, Nong Bua Lumphu Province. However, the serpentinite is only exposed near the center of an anomaly, so the large magnetic anomaly suggests that serpentinite is present below the meta-sedimentary rock types that are generally weakly magnetic.

## Magnetic Interpretation Related to Structural Features

The anomalies display several trends defined by alignment of gradients and shapes of anomalies, and are best illustrated in Figs. 5 and 6. The most dominant trend or lineament is in the northeast-southwest direction, followed by the northwest-southeast lineament, and the least dominant one is in a north-south direction.

The northwest-southeast trending lineaments are cross-cut by the northeast-southeast trending faults with sinistral movement and a horizontal slip of about 500 m[17]. As seen in the central domain, the northeast-southwest trending lineaments are younger than those of the northwest trends. The north-south trending lineaments mostly indicate major strike-slip faults in the eastern domain and the east-dipping thrust faults in the central domain (as the C1 sub-domain). The western domain is mainly represented by minor north-south trending lineaments and geophysical trends.

The newly processed of AEM data (see Figs. 4C and D) show the long continuity of lineaments of the moderate to high amplitude anomalies with the roughly north-south direction in the C1 sub-domain, corresponding to the thrust fault in the geologic maps[2, 3]. This result is in good agreement with the structure studied by Galong and Tulayatid[9], which showed the correlation of a conductor with the thrust fault from

the geological map. Additionally, the aeromagnetic study by Rangubpit[10] in Ban Yuak and Ban Sup, located in the southern part of the central domain, show the multiple thrust faults in this location. In contrast with this study, there is only one major thrust fault (TF2) that can be observed at this location. This is due to the smaller scale applied in this study. However, our studies show that the other thrust faults (TF1, 3, 4, and 5) in Figs. 5 and 6 are parallel to this thrust fault (TF2). Interestingly, the region faults that have been mapped using AEM data particularly nos. TF2, 3, 4 and 5, represented a very shallow source down-faulted beneath the only sedimentary rocks. Additionally, because of a parallel magnetic contour pattern and magnetic modeling (Fig. 7), the thrust faults in this area are indicated to have east dipping geometries.

In the northern parts of the central domain (the C3-sub-domain), narrow magnetic highs are related to Carboniferous mafic volcanic rocks (Carboniferous basalt and andesite) surrounded by Mid-Paleozoic chert and limestone, and crosscut by the sharp and distinct northeast faults. The regional magnetic anomaly amplitude of this zone is distinctively higher than those of the other sub-domains in the central domain. This high anomaly corresponds to MORB and oceanic island–arc lavas reported by Panjasawatworng *et al.*[6]. This zone is, therefore, interpreted to have formed in a volcanic island arc in the Devonian to Carboniferous[17].

Fault and fracture zones at or near surfaces are generally expressed as linear magnetic lows because of the alteration of magnetite to more weakly magnetic minerals at low temperature, high oxygen pressure in the presence of water. In contrast, the faults occurring at depth within the crust at higher temperature and high water vapour pressure, Fe-bearing hydrous silicates (biotite) form in the fault zone. Therefore, the associated fault is expressed by increased Fe-oxides (magnetite), which show strongly linear magnetic trends[21]. In this study, the TF1 thrust fault is associated with the positive anomaly, so we believe that the fault is a deeply seated structure that originated in a Permian-Triassic subduction system that accreted the crust in the study area[17]. The TF1 boundary has been adopted as the suture zone or tectonic line (called the 'Loei suture') described by Charusiri *et al.*[13]. The interpretation in this study suggests that this zone is a tectonically collision zone between the island arc and the Indochina continent. The collision zone is visible as regional and local shear zones shown as magnetic minima boundaries (the C1 sub-domain), and marks the accretionary boundaries of arc terrains. The collision zone is covered by Middle Paleozoic (?) metamorphic rocks that were broken by numerous collision-related wedge-shaped thrusts and faults. On the magnetic map, the eastern domain is the profound magnetic maximum where a significant component is due to magnetite enriched in serpentinites. It is possible that the serpentinites have been squeezed into wedge-shaped fractures within the sediment accretionary prism. In addition, the TF1 may be formed as a fault zone evidenced by magnetic modeling and may be a controlling structure throughout the geologic history of the area. Moreover, the northwest-southeast trending fault systems seem to change their orientation to north-south trending, especially in the northern part of the study area. This is probably due to a major change in tectonic stress and orientation, perhaps leading to the clockwise rotation of Southeast Asia by Indo-Australia collision[12, 13].

Within the eastern domain, the magnetic trends are characterized by a rather irregular pattern of magnetic anomalies containing the long segments with predominant northwestern and northern trends. This domain shows the north-south shear zone in the E1 sub-domain as indicated by en-echolon features of high magnetic intensity. These imbrications may be caused by the compressive tectonic stress roughly in the north-south direction due to the subduction of the oceanic slab beneath the amalgamated, mainland Southeast Asia terrain[7]. Moreover, this domain contains a set of the northwest-southeast lineaments that cut the shear zones and the TF1 and TF2 thrust faults in the north part of the domain, conforming a younger sinistral strike-slip motion. The magnetic data also show that the domain consists of several discontinuous, sinistrally side-stepping lineaments. This domain is represented by a zone of high strain, which may be influenced by the tectonic collision in this area.

In general, there is a good correlation between exposed geologic units and the aeromagnetic anomalies, with many of the mapped faults displaying a strong magnetic signature. Moreover, a number of magnetic anomalies strongly suggest that a number of significant faults are not shown on the existing geologic map. In some places, faults mapped on the surface have no magnetic expression and cut across magnetic features.

Comparison of the magnetic lineaments with the geologic map[2, 3] (Fig. 8A) show that many of the magnetic anomaly trends (red color) coincide with geological contacts or faults (black color) or closely parallel them. Some poor correlations in the northeast-southwest trending faults contrast strongly in the central domain and the major north-south trending faults in the eastern domain, where they were not found on the geological map. Good correlation with the northeast-southwest trending fault segments in the eastern and central domains are observed in both magnetic lineaments and boundaries on the existing geological maps. Comparison of the major lineaments from Landsat TM5[7] (cyan color) and aeromagnetic lineament (red

color) maps (Fig. 8B) shows that the mapped lineaments have similar trends, but the locations are mostly in parallel, suggesting that the sources of the two types of anomalies are different in depths. Additionally, the coincidence of the northeast-southwest trending faults in the central domain of the aeromagnetic image and the Landsat image[7] likely indicate that these faults are associated with the shallow fault sets that continue across the Loei basin, but these lineaments are not shown on the geological maps.

Large-scale, open and upright folds dominated the central domain, are obvious in magnetic, electromagnetic and Landsat images. The southern part of the eastern domain is a zone of steeply dipping and tightly folded sub-domains consisting of sedimentary and serpentinite rocks, and defining an area with high magnetic intensities. The dominant northwest to north trends are clearly visible as the magnetic lineaments surrounding axial surfaces (green color in Fig. 8) of the fold structures. However, the difference of axial plane orientations in the E4 sub-domain, with north and northeast trends, suggests two stages of folding. The first stage probably occurred as compressive stress developed in a roughly east-west direction, and the second stage took place as the northeast-southwest trending compressive stress. This result corresponds with that of Neawsuparp and Charusiri[7] for a major change in tectonic regime during the India-Asia collision.

## CONCLUSIONS

Based on our aeromagnetic interpretation, the Loei area is divided into three magnetic domains; namely eastern, central and western domains. The eastern domain is represented by mainly high magnetic intensities with major strike-slip faults and small folds. The central domain consists of low magnetic intensities, thrust faults, large open synclinal fold and small tight anticlinal folds. The western domain contains the large and prominent circular features with moderate magnetic intensities and north-south trending lineaments.

Three main suites of the magnetic lineaments are identified including northeast-southwest, northwest-southeast and north-south trending features. In the central domain, the northwest-southeast trending lineaments are cross-cut by the northeast-southwest trending lineaments, indicating that the northeast-southwest trending lineaments are younger than those of the northwest-southeast trends. Additionally, the northwest-southeast trending lineaments in the central domain represent major thrust faults. The north-south trending lineaments in the eastern part of the area are regarded as major strike slip faults. Some magnetic

lineaments correspond to previous mapped faults, and several interpreted lineaments are previously unknown faults.

Our geophysical interpretation was developed to give more details on the covered bedrock in the Loei area. The recently complied geophysical interpretation of the Loei area is highly useful for studying the anomalous composition and Paleotectonic crust in the Loei area that has been formed by arc-continent collision in the Paleozoic time.

## REFERENCES

1. Chareonpawat A, Wongwanit T, Tantiwanit V and Kitiprariwat A (1975) Geological map of sheet Changwat Loei (NE 47-12) scale 1:250,000. Geological Survey Division, Department of Mineral Resources, Thailand.
2. Mineral Resources Development Project (MRDP) (1988) Geology of Loei area. Geological Complication and Editing Section, Geological Research and Technology Geological Survey Division, Bangkok, Department of Mineral Resources, Thailand, 61 p.
3. Chairangsee C, Hinze C, Machareonsap S, Nakornsri N, Silpalit M and Sinpool-Anunt S (1990) Geological map of Thailand 1:50,000: Explanation for the sheets Amphoe Pak Chom 5345 II, Ban Na Kha 5344 I, Ban Huai Khop 5445, King Amphoe Nam Som 5444 IV. Hannover: Geologisuhes Jahrbuch, Reihe B, 55p.
4. Intasopa S and Dunn T (1993) Petrology and Syn-Nd isotropic systems of the basalts and rhyolites, Loei, Thailand. Journal of Southeast Earth Sciences, **9**,167-80.
5. Charusiri P (1989) Lithophile metallogenetic epochs of Thailand: A Geological and Geochronological Investigation. Ph.D Thesis, Queen's University, Canada, 819 p.
6. Panjaswatwong Y, Chantaramee S, Limtrakun P and Pirarai K (1997) Geochemistry and tectonic setting of eruption of central Loei volcanic in the Pak Chom area, Loei, northeast Thailand. The International Conference on Stratigraphy and Tectonic Evolution of Southeast Asia and the South Pacific, pp. 287-302. Aug.19-24, Bangkok, Thailand.
7. Neawsuparp K and Charusiri P (2000) Lineament analysis from Landsat data for structural geology and mineral occurrences in Loei area, Northeastern Thailand. In Proceedings of the International Conference on Applied Geophysics, November 9-10, 2000, Chiang Mai, Thailand.
8. Seusutthia K and Maopeth N (2001) Petrography and geochemistry of ultramafic rocks at Ban Bun Tan, Suwan Khuha Sub-district, Nong Bua Lumphu Province. Department

of Geology, Chulalongkorn University, Bangkok, Thailand, 84 p (unpublished).

9.  Galong W and Tulyatid J (1992) Airborne geophysical data interpretation of eastern Loei area: An aid for Geological mapping and mineral exploration. In C. Piancharoen (ed.),Proceedings of National Conference on Geological Resources of Thailand: Potential for Future Development, pp. 70-85. November 17-24, Department of Mineral Resources, Bangkok, Thailand.

10. Rangubpit W (2003) Image Processing and Interpretation of Aeromagnetic and Resistivity Data over Two 1:50,000 Map Sheet Area of Ban Yuak and Ban Sup, Loei area, Thailand. M.Sc. Thesis, University of New South Wales, Australia (unpublished).

11. Neawsuparp K, Charusiri P and Meyers J (2004) Application of aeromagnetic data and GIS integration for mapping continuity of geotectonic feature in the Loei area , Northeast Thailand. In Proceedings of RPJ-Ph.D. Congress V, The Thailand Research Fund , April 23-25, Chonburi, Thailand, p 85.

12. Bunopas S (1992) Regional stratigraphic correlation in Thailand. Proceeding of the National Conference on Geologic and Mineral Resources of Thailand: Potential for Future Development, November 17-24, Department of Mineral Resources, Bamgkok, Thailand, pp.189-208.

13. Charusiri P, Daorerk V, Archibald D, Hisada K and Ampaiwan T (2002) Geotectonic evolution of Thailand: A New Synthesis. Journal of the Geological Society of Thailand No.1,1-20,2002: pp.1-20.

14. Bunopas S (1988) Summary of geology of Loei area and accompanying 1:100,000 Geological map. Mineral Resources Development Project, Department of Mineral Resources, Thailand, 61 p.

15. Putthapiban P (2002) Geology and Geochronology of igneous rocks of Thailand. In the Proceedings of the Symposium on Geology of Thailand, 26-31 August 2002, Department of Mineral Resources, Bangkok, Thailand, pp. 261-83.

16. Nakapadungrat S and Putthapiban P (1992) Granites and associated mineralization in Thailand. In the proceedings of the National Conference on Geologic Resources of Thailand: Potential for Future Development, Department of Mineral Resources, November 17-24. Bangkok, Thailand.

17. Neawsuparp K (2005) Application of Airborne Geophysical and Remote Sensing Data to Structural Geology and Tectonic Setting in Loei Area, Northeastern Thailand. Ph.D. Thesis, Department of Geology, Chulalongkorn University, Bangkok, Thailand. (unpublished).

18. Milligan P R and Gunn P J (1997) Enhancement and presentation of airborne geophysical data. Journal of Australian Geology & Geophysics, **17**(2), 63-76.

19. Gunn P J (1997) Quantitative methods for interpreting aeromagnetic data. JGSO Journal of Australian Geology and Geophysics, **17**(2), 105-14.

20. Safon C, Vasseur G and Creu M (1977) Some application of linear programming to the inverse gravity problem. Geophysics, **42**, 1215-99.

21. Airo M-L and Ruotoistenmaki T (2000) Magnetic signatures of finish bedrock and their relationship with geological boundaries. In: Pesonen, L., Korja, A. and Hjelt, S-E. (editors): Lithosphere 2000. Report S-41, Institute of Seismology, University of Helsinki, Finland,(abstract).

22. Fontaine H and Ingavat R (1982) The Lower Carboniferous in Thailand. In Proceedings of the10[th] International Stratigraphy Geology Carboniferous Congress, Madrid 1983, 1:129-132, Madrid 21.

23. Plijm B A and Marshak S (1997) Earth Structure, an Introduction to Structural Geology and Tectonics. WCB/McGraw-Hill, New York, 495 p.

24. Telfold W M, Geldart L P, Sheriff R E and Keys D A (1986) Applied Geophysics. Cambridge University Press, New York, 860 p.

25. Whitaker A (1994) Integrated geological and geophysical mapping of southwestern Western Australia. Australian Geological Survey Organisation, Journal of Geology and Geophysics **15**, 313-28.